ISSN 2616-5880 Vol. 6, Issue 3: 71-78, DOI: 10.25236/AJMC.2025.060310

Study on Arrhenius Constitutive Model of Ti-22Al-24Nb-0.5Mo Alloy Based on Strain Compensation

Liye Xie[1,a], Xueyan Jiao[1,2,*]

[1]*School of Naval Architecture and Port Engineering, Shandong Jiao Tong University, Weihai, Shandong Province, 264209, China*
[2]*Jinma Industrial Group Co., Ltd All Rights Reserved, Rizhao, 276800, China*
[a]*15763376034@163.com*
[*]*Corresponding author: jiaoxueyan@sdjyu.edu.cn*

Abstract: *Tensile tests at elevated temperatures were performed on the Ti-22Al-24Nb-0.5Mo alloy using an MTS universal testing machine to investigate its hot deformation behavior. The experiments were conducted at temperatures ranging from 875 to 950 ℃ and strain rates of 0.001 to 0.55 s^{-1}. Flow stress-strain curves of the alloy were obtained under these conditions, and the effects of deformation temperature and strain rate on flow stress were analyzed. A fifth-order polynomial was used to model the relationship between strain and various material parameters, achieving a correlation coefficient (R) greater than 0.99. An Arrhenius type constitutive model with strain compensation was established. The calculated results demonstrated a correlation coefficient of 0.994 between the predicted and experimental flow stress values, with an average relative error of 4.24%. This confirms the model's high accuracy, making it suitable for numerical simulations.*

Keywords: *Ti-22Al-24Nb-0.5Mo; Hot Deformation Behavior; Arrhenius Model; Strain Compensation*

1. Introduction

Ti_2AlNb-based alloys, classified as Ti-Al intermetallic compound, typically contain Ti-(18-30)Al-(12.5-30)Nb (at.%) with trace elements such as V, Mo, and Ta added for solid solution strengthening to enhance their mechanical properties [1-2].

Ti_2AlNb-based alloys can withstand prolonged service at 600 to 750°C, characterized by low density, high specific strength, and excellent oxidation resistance. These alloys are considered next-generation aerospace structural materials with broad application potential. However, their high forming temperatures and significant deformation resistance persistently hinder widespread industrial adoption. Consequently, reducing forming temperatures and deformation resistance has become a primary research focus, necessitating comprehensive analysis of the high temperature deformation behavior of Ti_2AlNb-based alloys to advance rational forming processes [3-5].

The constitutive model for material hot deformation characterizes the influence of deformation temperature, strain rate, and strain on the flow stress [6]. As a precise representation of material flow behavior, this equation critically determines the reliability and predictive capability of finite element simulations[7]. These constitutive models are broadly categorized into three types[8]: phenomenological models[9], physical models[10], and artificial neural network models [11]. The phenomenological Arrhenius model, in particular, is widely used to characterize the relationship among flow stress , strain rate, and deformation temperature in metallic materials during hot deformation [12-13]. Xia Yufeng [14] conducted isothermal compression experiments on a Ti-6Al-4V-0.1Ru alloy and established an Arrhenius type constitutive model applicable to both the (α+β) dual-phase and β single-phase regions. He further simulated the process using Deform-2D software. Li Hu [15] developed a strain-compensated Arrhenius model based on experimental true stress-strain data, implementing it using the UHARD subroutine in ABAQUS to analyze the hot deformation of a homogenized Mg-8.5Gd-2.5Y-0.8Zn-0.4Zr alloy. Lu Yupeng [16] studied the hot deformation behavior of a Ti2AlNb alloy through tensile tests at different strain rates and temperatures. He established a constitutive model for the Ti-22Al-25Nb alloy under these conditions and discussed the effect of temperature on the deformation activation energy in combination with microstructural evolution. However, the study did not consider the effect of strain on flow stress. Zhou Feng [17] performed isothermal compression tests on a Ti-22Al-24Nb-0.5Y alloy at constant strain rates using a Gleeble-3500 simulator. The data were corrected for friction and temperature effects to

ISSN 2616-5880 Vol. 6, Issue 3: 71-78, DOI: 10.25236/AJMC.2025.060310

establish a strain-compensated constitutive model.

Tensile tests were performed on a Ti-22Al-24Nb-0.5Mo alloy using an MTS universal testing machine at various deformation temperatures and strain rates. The resulting true stress-strain curves were obtained, and a constitutive equation was developed. A strain compensated Arrhenius constitutive model was established to accurately describe the influence of strain on the hot deformation behavior. This model provides critical insights for the subsequent hot forming processes and finite element simulations of this alloy.

2. Experimental materials and methods

In this study, a hot-rolled Ti-22Al-24Nb-0.5Mo alloy plate with a thickness of 2 mm was used as the original material. The nominal composition of the alloy is presented in Table 1. High-temperature tensile tests were conducted on an MTS universal testing machine. The geometry of the tensile specimen is shown in Figure 1; it had a gauge length of 15 mm. The tests were performed at deformation temperatures of 875, 900, 925, and 950 °C and at strain rates of 0.55, 0.1, 0.01, and 0.001 s^{-1}.

Table 1: Atomic Percentage of Ti-22Al-24Nb-0.5Mo Alloy (at. %)

	Ti (at %)	Al (at %)	Nb (at %)	Mo (at %)
Nominal composition	Bal.	22	24	0.5

Prior to the tensile test, the surface and sides of the specimen were polished. Its dimensions were measured, the gauge length was marked, and an anti-oxidant glass coating was applied. The prepared specimen was placed into the furnace after the furnace had reached the target temperature. The specimen was held at that temperature for 5 minutes to stabilize before the tensile test began at a constant strain rate. The test continued until fracture occurred. Subsequently, the fractured specimen was immediately removed from the furnace and water-cooling.

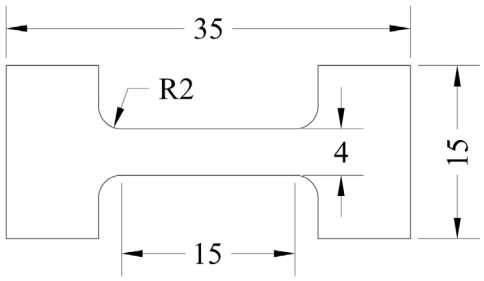

Figure 1: Dimensions of high temperature tensile test specimens for Ti-22Al-24Nb-0.5Mo alloy, (unit, mm)

3. Analysis of experimental results

Figure 2 shows the real stress-true strain curve of the Ti-22Al-24Nb-0.5Mo alloy obtained from the high temperature tensile tests. It can be observed that at a constant temperature, the flow stress decreases as the strain rate decreases, while the fracture elongation increases. For instance, at 875 °C and a strain rate of 0.55 s^{-1}, the tensile strength reaches 450 MPa, whereas it is only 175 MPa at a strain rate of 0.001 s^{-1}. This indicates that the alloy exhibits positive strain rate sensitivity. Furthermore, when the strain rate is held constant, the flow stress decreases with increasing temperature. For example, at a strain rate of 0.1 s^{-1}, the tensile strength is 360 MPa at 875 °C and decreases to 310 MPa at 900 °C, demonstrating negative temperature sensitivity.

The overall shape of the stress-strain curve can be divided into four distinct stages [18]. In the initial stage, the stress increases rapidly with increasing strain during deformation, leading to a substantial rise in dislocation density within the alloy. This results in the formation of numerous dislocation tangles, along with the emergence and proliferation of subgrain boundaries. In the second stage, after reaching the peak stress, the material undergoes a prolonged period of stable deformation. The interplay between work hardening and dynamic softening results in a relatively steady or linearly decreasing flow stress. The third stage is the necking stage, where the stress decreases rapidly with strain. Deformation transitions from being uniform to highly localized. This localization leads to a reduction in load-bearing capacity, resulting in necking and ultimately fracture.

ISSN 2616-5880 Vol. 6, Issue 3: 71-78, DOI: 10.25236/AJMC.2025.060310

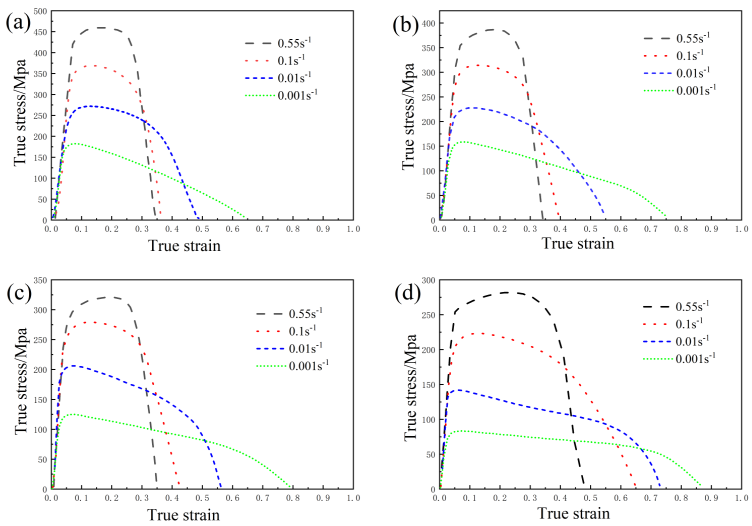

Figure 2: Flow stress-strain curves at various deformation temperatures during high temperature tensile testing of the Ti-22Al-24Nb-0.5Mo alloy. (a)875℃ (b)900℃ (c)925℃ (d)950℃

4. Establishment and revision of constitutive models

4.1 Establishment of the Arrhenius constitutive model

The Arrhenius equation is widely used to characterize the deformation behavior of metallic materials at elevated temperatures, as it describes the relationship between flow stress, temperature, and strain rate. Accurate prediction of flow stress is essential for predicting hot deformation behavior and for ensuring reliable finite element simulation results.

$$\dot{\varepsilon} = A_1 \sigma^{n_1} exp\left[-\frac{Q}{RT}\right] \quad (\alpha\sigma < 0.8) \tag{1}$$

$$\dot{\varepsilon} = A_2 exp(\beta\sigma) exp\left[-\frac{Q}{RT}\right] \quad (\alpha\sigma > 1.2) \tag{2}$$

$$\dot{\varepsilon} = A\left[sinh(\alpha\sigma)\right]^n exp\left[-\frac{Q}{RT}\right] \quad (all\ \sigma) \tag{3}$$

In Equations (1) to (3): $\dot{\varepsilon}$ is the strain rate, s^{-1}; σ is the flow stress, MPa; Q is the hot deformation activation energy, ($J \cdot mol^{-1}$); R is the gas constant, $R = 8.314$ J/(mol·K); T is the deformation temperature, K; A_1, A_2, A, n_1, n, β, and α are material constants, and satisfy the relationship $\alpha=\beta/n_1$.

At the same time, the Zener-Hollomon parameter [19] (also known as temperature compensated strain rate) is introduced to describe the effects of temperature and strain rate on stress, as shown in Equation (4). By taking the logarithm of both sides of Equations (1) through (3), Equations (5) through (7) can be obtained.

$$Z = \dot{\varepsilon} exp(\frac{Q}{RT}) = A[sinh(\alpha\sigma)]^n \tag{4}$$

$$ln\dot{\varepsilon} = lnA_1 + n_1 ln\sigma - \frac{Q}{RT} \tag{5}$$

$$ln\dot{\varepsilon} = lnA_2 + \beta\sigma - \frac{Q}{RT} \tag{6}$$

$$ln\dot{\varepsilon} = lnA + nln\left[sinh(\alpha\sigma)\right] - \frac{Q}{RT} \tag{7}$$

Under constant temperature conditions, Equation (8) can be obtained by taking the partial derivative of Equation (7)

ISSN 2616-5880 Vol. 6, Issue 3: 71-78, DOI: 10.25236/AJMC.2025.060310

$$n = \frac{\partial \ln \dot{\varepsilon}}{\partial ln\left[sinh\left(\alpha\sigma\right)\right]} \tag{8}$$

Under constant strain rate conditions, Equation (9) can be obtained by taking the partial derivative of Equation (7).

$$Q = nR\frac{\partial ln\left[sinh\left(\alpha\sigma\right)\right]}{\partial\left(1/T\right)} \tag{9}$$

Likewise, graph the relationship curves for *lnε̇-ln[sinh(ασ)]* and *ln[sinh(ασ)]-1/T*, as depicted in Figures 3(c) and (d). The mean value of n is 4.7122, the mean value of $\frac{\partial ln[sinh(\alpha\sigma)]}{\partial(1/T)}$ is 15174.74, and Q= 594505.58 J/mol.

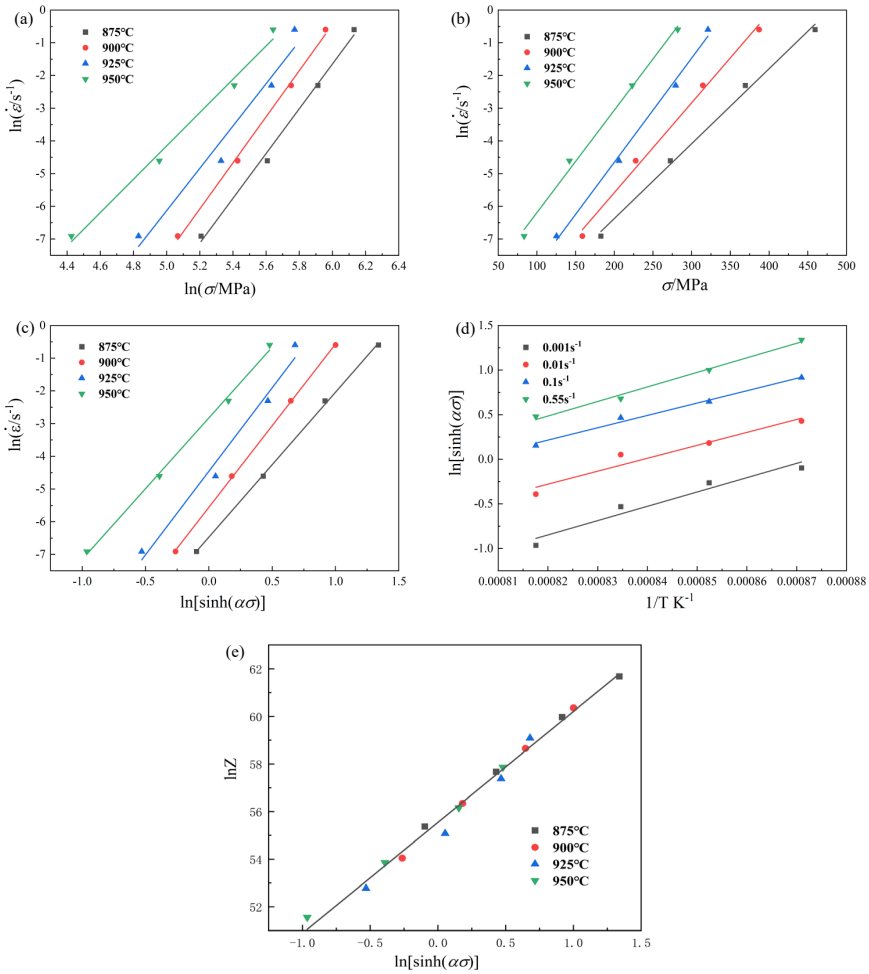

Figure 3: (a) lnε̇-lnσ, (b) lnε̇-σ, (c) lnε̇-ln[sinh(ασ)], (d) ln[sinh(ασ)]-1/T, (e) lnZ-ln[sinh(ασ)] fitting relationship diagram

The amalgamation of Equations (3) and (4) results in *lnZ=lnA+nln[sinh(ασ)]*. Plotting *lnZ-ln[sinh(ασ)]* and fitting the data, as seen in Figure 3(e), results in an intercept of *lnA=55.54*, $A=1.32747\times10^{24}$. In summary. The Arrhenius peak stress constitutive model for the Ti-22Al-24Nb-0.5Mo alloy is summarized as follows:

$$\dot{\varepsilon} = 1.32747\times10^{24}\left[sinh\left(0.00446\sigma\right)\right]^{4.7122} exp\left(\frac{-594505.58}{8.314T}\right) \tag{10}$$

Similarly, using the test data at different deformation temperatures and strain rates, a true strain range of 0.08 to 0.26 in the plastic stage was selected. Points were taken at intervals of 0.03 true strain to calculate α, n, Q, and lnA following the aforementioned method. The results are presented in Table 2.

ISSN 2616-5880 Vol. 6, Issue 3: 71-78, DOI: 10.25236/AJMC.2025.060310

Table 2: Constitutive equation parameters under different true strains

ε/s^{-1}	α/MPa^{-1}	n	$Q/(J\cdot mol)$	lnA
0.08	0.004643	4.9534	569915.57	52.950
0.11	0.004590	4.7002	607781.28	56.812
0.14	0.004591	4.5119	588203.07	54.884
0.17	0.004617	4.3782	570769.58	53.124
0.20	0.004667	4.2655	543367.50	50.357
0.23	0.004750	4.2040	520560.73	48.175
0.26	0.004934	4.2549	494073.99	45.484

4.2 Constitutive model correction based on strain compensation

The Arrhenius equation fails to consider the influence of strain on material parameters during deformation. Consequently, strain compensation was incorporated into the Arrhenius equation to develop a revised constitutive model. Subsequently, polynomial fitting was performed on the obtained material parameters. The fifth-order polynomial provided the best fit and was therefore selected. Thus, the relationships between the material parameters *α, n, Q, lnA* and true strain are expressed by fifth-order polynomials, as given in Equations (11)-(14). The corresponding fitting coefficients are listed in Table 3.

$$\alpha(\varepsilon) = B_0 + B_1\varepsilon + B_2\varepsilon^2 + B_3\varepsilon^3 + B_4\varepsilon^4 + B_5\varepsilon^5 \tag{11}$$

$$n(\varepsilon) = C_0 + C_1\varepsilon + C_2\varepsilon^2 + C_3\varepsilon^3 + C_4\varepsilon^4 + C_5\varepsilon^5 \tag{12}$$

$$Q(\varepsilon) = D_0 + D_1\varepsilon + D_2\varepsilon^2 + D_3\varepsilon^3 + D_4\varepsilon^4 + D_5\varepsilon^5 \tag{13}$$

$$\ln A(\varepsilon) = E_0 + E_1\varepsilon + E_2\varepsilon^2 + E_3\varepsilon^3 + E_4\varepsilon^4 + E_5\varepsilon^5 \tag{14}$$

Table 3: Polynomial Fitting Coefficients

Material parameters	α	n	Q	lnA
Coefficient	B_0=0.00508	C_0=5.77791	D_0=-899073.189	E_0=-88.989
	B_1=-0.00644	C_1=-6.28853	D_1=45007096.086	E_1=4309.589
	B_2=-0.02339	C_2=-138.97057	D_2=-516766068.479	E_2=-48903.410
	B_3=0.69561	C_3=1556.48446	D_3=2868962813.615	E_3=268019.998
	B_4=-3.51402	C_4=-6332.61434	D_4=-7824201628.945	E_4=-721551.190
	B_5=5.84526	C_5=9332.56173	D_5=8378391289.439	E_5=762928.669
R^2	0.99993	0.99997	0.99748	0.99725

The relationship between the material parameters and strain is shown in Figure 4.

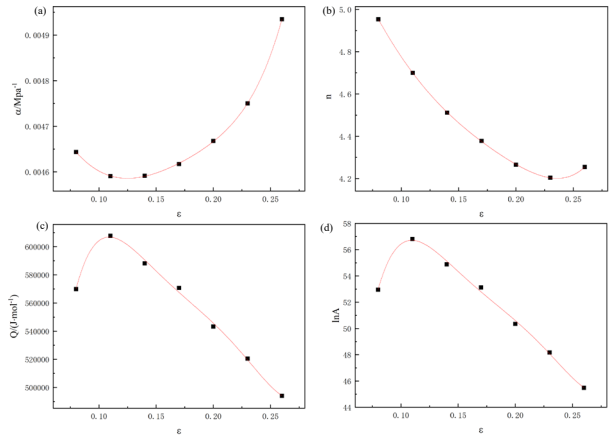

Figure 4: Polynomial fitting curves between different material parameter values and true strain

Substituting Equations (11) to (14) into Equation (4) yields the Arrhenius constitutive model Equation (15) for the Ti-22Al-24Nb-0.5Mo alloy based on strain compensation.

ISSN 2616-5880 Vol. 6, Issue 3: 71-78, DOI: 10.25236/AJMC.2025.060310

$$\sigma_{(\varepsilon)} = \frac{1}{\alpha(\varepsilon)} ln\{\frac{Z(\varepsilon)}{A(\varepsilon)})^{\frac{1}{n(\varepsilon)}} + [(\frac{Z(\varepsilon)}{A(\varepsilon)})^{\frac{2}{n(\varepsilon)}} + 1]^{\frac{1}{2}}\} \tag{15}$$

In Equation (15):

$$Z(\varepsilon) = \dot{\varepsilon} exp\left(\frac{Q_{(\varepsilon)}}{RT}\right) \tag{16}$$

4.3 Validate model Constitutive model validation

To validate the accuracy of the aforementioned strain-compensated Arrhenius constitutive model, the flow stress under various deformation conditions was computed using Equation (15) and compared against the experimental data, as shown in Figure 5.

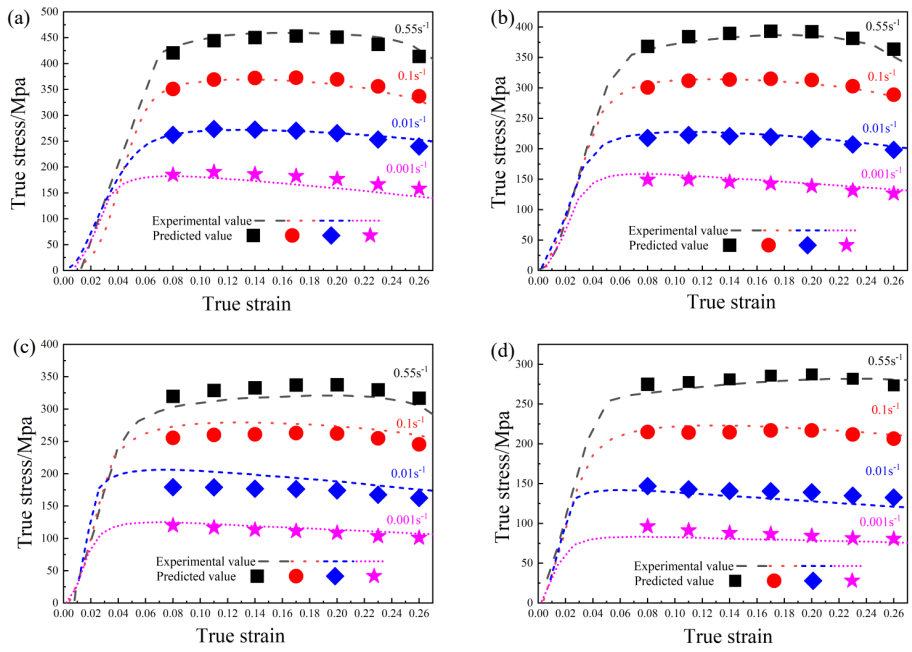

Figure 5: Experimental and predicted values of flow stress for Ti-22Al-24Nb-0.5Mo alloy at different deformation temperatures. (a)875 ℃(b)900 ℃(c)925 ℃(d)950 ℃

Furthermore, the linear correlation coefficient (R) and average absolute relative error ($AARE$) [20] are used to calculate the deviation between the model's flow stress and the experimental test data, thereby evaluating the reliability of the model. The equations for calculating R and $AARE$ are as follows:

$$R = \frac{\sum_{i=1}^{N}(E_i - \bar{E})(P_i - \bar{P})}{\sqrt{\sum_{i=1}^{N}(E_i - \bar{E})^2 \sum_{i=1}^{N}(P_i - \bar{P})^2}} \tag{17}$$

$$AARE = \frac{1}{N}\sum_{i=1}^{N}\left|\frac{P_i - E_i}{E_i}\right| \times 100\% \tag{18}$$

In Equations (17) and (18), E_i and P_i denote the experimentally measured values and model predicted values of flow stress, respectively; $\bar{E}$ and $\bar{P}$ signify the mean values of experimental and model predicted flow stress, respectively; N indicates the number of analyzed and compared data sets. Figure 6 illustrates a determined correlation coefficient of 0.994, with an absolute average relative error of 4.24%.

ISSN 2616-5880 Vol. 6, Issue 3: 71-78, DOI: 10.25236/AJMC.2025.060310

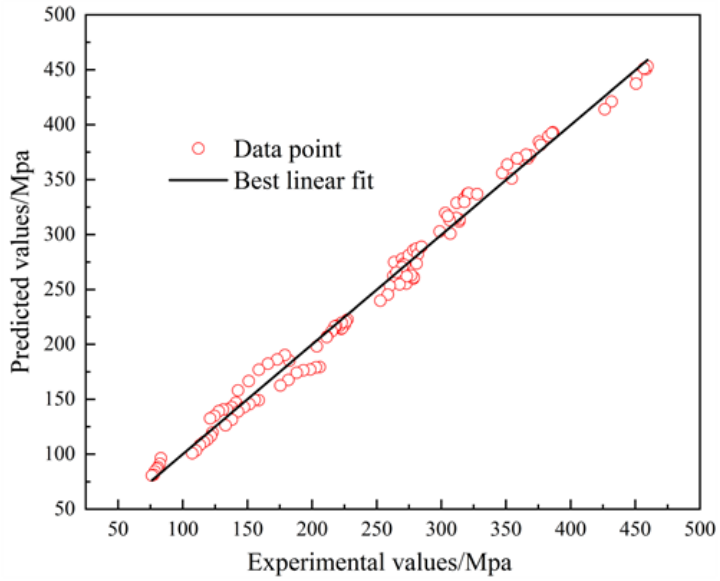

Figure 6: Correlation between predicted and experimental values for flow stress

5. Conclusion

1) The flow stress of Ti-22Al-24Nb-0.5Mo alloy is sensitive to deformation temperature and strain rate. When the deformation temperature is constant, the flow stress of the material increases as the strain rate increases. When the strain rate is constant, the flow stress of the material decreases as the deformation temperature increases.

2) The Arrhenius constitutive model parameters α, n, Q, and lnA for the Ti-22Al-24Nb-0.5Mo alloy are associated with strain ε. A fifth-order polynomial regression was employed to establish the correlation between strain and material parameters. The fitted material parameter curves demonstrate strong correlation, with coefficients surpassing 0.99. A strain compensation based Arrhenius constitutive model was developed for the Ti-22Al-24Nb-0.5Mo alloy. The precision of the constitutive model was assessed utilizing the correlation coefficient R and the average relative error $AARE$. The computed values were R = 0.994 and $AARE$ = 4.24%, indicating the high predictive accuracy of the model.

Acknowledgements

This project is supported by the National Natural Science Foundation of China (Grant No. 52205391), and Postdoctoral Innovation Program of Shandong Province (Grant No. SDCX-ZG-202400233).

References

[1] Li Baoyong. High temperature forming technology and equipment for lightweight structure of Ti-22Al-24Nb-0.5Mo alloy[D]. Harbin Institute of Technology, 2021.
[2] Liu Shishuang, Cao Jingxia, Zhou Yi, et al. Research and prospect of Ti_2AlNb alloy[J]. The Chinese Journal of Nonferrous Metals, 2021, 31(11): 3106-3126.
[3] Yang Jianlei, Zeng Ting, Wang Guofeng, et al. High Temperature Deformation Constitutive Equation for Ti-22Al-25Nb Alloy Fabricated by Powder Metallurgy[J]. Hot Working Technology, 2019, 48(04): 43-47.
[4] Du Gang, Cui Linlin, Lei Qiang, et al. Research and Development of Orthorhombic Titanium Aluminide[J]. Materials China, 2018, 37(01): 68-73.
[5] Lin P, He Z, Yuan S, et al. Tensile deformation behavior of Ti-22Al-25Nb alloy at elevated temperatures[J]. Materials Science & amp; Engineering A, 2012, 556617-556624.
[6] Liu Q, Wang Z, Yang H, et al. Hot Deformation Behavior and Processing Maps of Ti-6554 Alloy for Aviation Key Structural Parts[J]. Metals, 2020, 10(6): 828.
[7] Paturi R M U, Narala R K S. Constitutive flow stress formulation for aeronautic aluminum alloy AA7075-T6 at elevated temperature and model validation using finite element simulation[J].

ISSN 2616-5880 Vol. 6, Issue 3: 71-78, DOI: 10.25236/AJMC.2025.060310

Proceedings of the Institution of Mechanical Engineers, Part L: Journal of Materials: Design and Applications, 2016, 230(6): 994-1004.
[8] Lin Y, Chen X. A critical review of experimental results and constitutive descriptions for metals and alloys in hot working[J]. Materials & amp; Design, 2011, 32(4): 1733-1759.
[9] Li Jingdan, Li Rongbin, Liang Hongyu. Modification of Constitutive Model of SA508-3 Steel Based on Strain Compensation[J]. Hot Working Technology, 2024, 53(11): 134-137.
[10] Wu Y, Wang D, Liu Z, et al. A unified internal state variable material model for Ti_2AlNb-alloy and its applications in hot gas forming[J]. International Journal of Mechanical Sciences, 2019.
[11] Shi Wenpeng, Sun Cenhua, Li Jiajun, et al, 9310 Steel Constitutive Model Optimization Based on Artificial Neural Network Intelligent Algorithm[J]. Journal of Netshape Forming Engineering, 2024, 16(03): 171-180.
[12] Sellars C M, Mctegart W J. On the mechanism of hot deformation[J]. Acta Metallurgica, 1966, 14(9): 1136-1138.
[13] Rare Metals; Reports Outline Rare Metals Study Findings from Central South University (Hot Compression Deformation Behavior of Biomedical Ni-ti Alloy)[J]. Mining & amp; Minerals, 2019,
[14] Xia Yufeng, Jiang Wei, Cheng Qian, et al. Hot deformation behavior of Ti-6Al-4V-0.1Ru alloy during isothermal compression[J]. Transactions of Nonferrous Metals Society of China, 2020, 30 (01): 134-146.
[15] Li H, Mengwei L, Laixin S, et al. Study on hot deformation behavior of homogenized Mg-8.5Gd-4.5Y-0.8Zn-0.4Zr alloy using a combination of strain-compensated Arrhenius constitutive model and finite element simulation method[J]. Journal of Magnesium and Alloys, 2023, 11(3): 1016-1028.
[16] Lu Yupeng, Meng Lingjian, Yin Hongliang, et al. Constitutive Models for Tensile Deformation Behavior of Ti-22Al-25Nb Alloy Sheet at Elevated Temperatures[J]. Rare Metal Materials and Engineering, 2023, 52(03): 785-790.
[17] Zhou Feng, Wang Kelu, Lu Shiqiang, et al. Flow behavior and BP neural network high temperature constitutive model of Ti-22Al-24Nb-0.5Y alloy[J]. Journal of Materials Engineering, 2019, 47(08): 141-146.
[18] He Z, Wang Z, Lin P. A Comparative Study on Arrhenius and Johnson-Cook Constitutive Models for High-Temperature Deformation of Ti_2AlNb-Based Alloys[J]. Metals, 2019, 9(2): 13.
[19] Zener C, Hollomon J H. Effect of Strain Rate Upon Plastic Flow of Steel[J]. Journal of Applied Physics, 1944, 15(1): 22-32.
[20] J. D, W. L C, Y. B C, et al. Arrhenius constitutive model of FV520B steel[J]. Metalurgija, 2024, 63(1): 93-96.